CHEMICAL ENGINEERING TRANSACTIONS
VOL. xxx, 2024
A publication of AIDIC
The Italian Association of Chemical Engineering
Online at www.cetjournal.it
Guest Editors: Valerio Cozzani, Bruno Fabiano, Genserik Reniers

ISBN 979-12-81206-11-3; **ISSN** 2283-9216

A Modelling Approach for the Seismic Fragility Assessment of Process Towers

Antonio Vitale*[,a], Georgios Baltzopoulos[a], Della Corte Gaetano[a], Iunio Iervolino[a,b]

[a]Dipartimento di Strutture per l'Ingegneria e l'Architettura, Università di Napoli Federico II, Via Claudio 21, 80125 Naples, Italy.
[c]IUSS Scuola Universitaria Superiore di Pavia, Piazza della Vittoria 15, 27100 Pavia, Italy.
antonio.vitale5@unina.it

Process towers, whose purpose includes executing operations of mass transfer such as stripping, distillation, or liquid-liquid extraction, are usually constructed as vertical steel cylindrical pressurised shells, supported on a cylindrical skirt. Seismic risk analysts in an industrial setting, especially in NaTech context, are often faced with the issue that structural vulnerability models are not always available for the various industrial facilities. Process towers, although widespread, are one of those cases. The objective of the study presented in the paper is to simulate the behaviour of such towers when subjected to earthquake-induced ground shaking, with the goal of numerically deriving seismic fragility models. To this end, as a case study, two towers were considered with the same height and internal diameter, but different operating pressures, which determines the thickness of the pressure vessel and, consequently, the configuration of the anchorage system. For each of the two models, *multi-stripe* dynamic analysis was conducted, using a selection of *hazard-consistent* ground motion records, on *joystick* models. The results of the dynamic analyses are presented and their use for the derivation of fragility functions for certain damage states is discussed. This modelling strategy can contribute to streamline the fragility evaluation of such structures, given the variety of geometries which appear in industrial plants.

1. Introduction

Structural damage to even a single industrial unit may lead to a loss of contents that may potentially trigger any from a series of accidents, such as explosions, pool fires, or dispersion of toxic clouds, with consequences in terms of economic losses, human life, or environmental impact (Krausmann et al., 2011). One of the possible trigger causes of such technological accidents are natural hazards to which the plant is exposed, such as earthquakes, wind, floods or tsunamis, called NaTech events. Frameworks for quantitative risk assessments (QRAs) were developed by various authors. Particularly in the seismic domain, studies by Antonioni et al. (2007), Fabbrocino et al. (2005), and Iervolino (2003) analysed the consequences of seismic events on industrial facilities. However, the sheer structural diversity of each individual unit within a single plant poses a challenge in predicting the plant's overall response to a natural event. In fact, QRA employs fragility models to quantify the probability to content loss following structural damage, that not always are available for all individual units. The purpose of the study herein presented was to provide a summary of a study of process tower response under seismic action which is added to few existing works of literature, such as for example Karaferis et al. (2022) and Moharrami & Amini (2014). These towers are widely used in various industrial processes for physical separation, such as distillation or stripping. In this work, seismic fragility models were developed analytically for a set of towers assumed located in Ravenna (Italy). Thus, the case-study structures were partly designed in accordance with the EN 13445-3 (2021) European standard, based on *allowable stress design* via semi-empirical formulae, while design against wind and seismic actions was carried out according to the Italian building code (NTC, 2018). For this case study, two towers were considered with the same height and internal diameter but different internal pressure: $6\ bar$ and $80\ bar$ respectively. The towers were modelled using a nonlinear finite element model, analysing their response under a set of hazard-consistent ground motions via incremental dynamic analysis.

2. Case-study structures

Process towers are vertical steel structures made by a pressurised vessel resting welded on a skirt-type steel cylinder support. The pressure vessel is a cylindrical shell, closed off at the edges by two hemispherical ends. The skirt is a steel cylindrical shell without openings and is not pressurised. Typically, openings are present at different heights of the vessel to accommodate piping and circulation of the contents, but herein the attachments were excluded from the design and analysis. The supporting element of the tower, that is the steel skirt, is connected to the foundation via an annular base plate welded at its base and anchored to the concrete via anchor bolts. Process towers can have different internal configurations depending on the specific separation process. For the purposes of this study, it was assumed that trays are installed in the interior of the pressure vessel. These are perforated steel plates used in the separation process occurring during normal operating conditions. Figure 1-a) shows a schematic drawing of the facility examined in this paper, while the panel b) presents the detail of foundation connection designed using a simple bearing plate.

The case study includes two towers that have the same total height (H) and internal diameter (D_i) but different internal operating pressures (P), specifically $6\ bar$ and $80\ bar$. The design was carried out according to the semi-empirical formulae approach of the EN 13445-3 (2021) standard, and involves dimensioning thicknesses of the vessel (e_{col}), of the skirt (e_{skirt}) and of the base plate (e_4), as wells as the width of the base plate (b_1), and the number (n_b), diameter (d_b) and length (L_b) of the anchors, and other characteristics of the base plate such as the edge distance of the skirt (b_2) and the distance of the anchors from the skirt (b_3). While design standards prescribe minimum required thicknesses for the tower under internal operating pressure, these thicknesses must be further verified, and possibly revised, for other loading scenarios including both normal operating conditions (e.g., start-up, shutdown, and installation) and exceptional conditions. For the normal operating conditions, simultaneous external wind pressure was considered where necessary. On the other hand, exceptional design conditions correspond to low-probability events requiring a safe shutdown and inspection of the vessel in the aftermath. For these nominal load conditions, seismic actions were applied considering the vessel both pressurised and without internal pressure. To calculate the effects of wind and seismic actions, equivalent static analysis was performed. These actions were defined by considering the towers' location to be in a petrochemical plant situated in Ravenna (Italy). Wind loads were evaluated following the EN 1991-1-4 (2004) standard for long circular cylinders, incorporating the relevant national annex (NTC, 2018) provisions. Seismic action was applied to the structure using an inverse triangular distribution as prescribed by EN 1998-1 (2013). Seismic parameters were taken from the Italian building code (NTC, 2018) considering a collapse prevention limit state, corresponding to a return period of the seismic action $Tr = 1950\ y$, with a behaviour factor $q = 1$ (Brunelli & Borgognoni, 2014). The results of the design of the two towers, called Tower-1 with $P = 6\ bar$, and Tower-2 with $P = 80\ bar$, are summarized in Table 1.

To facilitate the comparative analysis, both towers were designed with the same base connection system, that is a simple annular bearing plate without steel stiffening elements, employing the same number of anchors. The design of Tower-1 resulted in a required quantity of structural steel, excluding pipes and connection detailing, weighing at 500 kN, while the corresponding value for Tower-2 turned out to be 5337 kN. Therefore, it appears that the difference in operating pressure between the two towers resulted in approximately tenfold material consumption for the structural members.

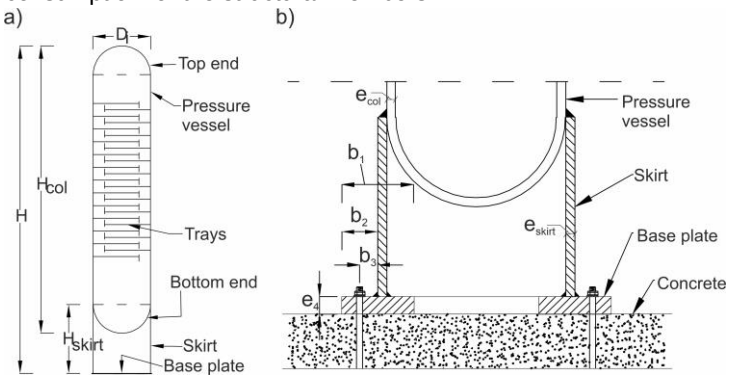

Figure 1: a) Schematic cross-section of a pressure vessel. b) Detailing of the foundation connection.

Table 1: Geometric features of the two process towers.

	P [bar]	H [m]	D_i [m]	H_{col} [m]	H_{skirt} [m]	e_{col} [mm]	e_{skirt} [mm]	e_4 [mm]	b_1 [mm]	b_2 [mm]	b_3 [mm]	n_b	d_b [mm]	L_b [mm]
Tower-1	6	25.6	4.5	22.5	5.4	12	8	25	135	90	45	24	24	25

Tower-2	80	200	30	100	360	240	120	90	836

3. Structural modelling and analysis

3.1 Model

Derivation of fragility models typically requires a numerical structural model, the selection of input ground motions, running dynamic analyses, and the evaluation of the structural response. The modelling approach herein uses a simple joystick-type multiple-degree-of-freedom model to predict the seismic response of the process towers via nonlinear time-history analysis. This model, shown in *Figure 2*-a), comprises two-node one-dimensional finite beam elements to represent the pressure vessel and supporting skirt, with intermediate nodes used for the discretisation of the structure's inertial properties. The base plate is modelled with rigid beam spokes, one per anchor, connecting the lowermost nodes of the tower structure with a series of nonlinear springs, whose force-displacement relationship represents the behaviour of the anchors and the annular base plate when the former are in tension and when the latter is in contact with the foundation. In fact, the strength and stiffness of the springs, representing the connection to the foundation, were evaluated by considering two components, that are the anchor bolt and base plate. The force-displacement relationship of the springs in tension was calculated considering the behaviour of the anchors in tension and the base plate in bending under the tension anchor force. On the other hand, the springs under compression model the bending behaviour of the base plate in contact with the concrete and the foundation concrete under compression. The elastic stiffnesses, the yielding strength in compression (F_1) and in tension (F_2) and ultimate tension (F_3) strengths of the springs were obtained following the equivalent T-stub method approach proposed by EN 1993-1-8 (2005). From these values, the yielding displacement in compression (δ_1) and in tension (δ_2) are obtained. Panel b) shows the behaviour in tension (first quadrant) and in compression (third quadrant) of the springs. The compression behaviour was modelled with an elastic-perfectly plastic force-elongation diagram, while the tension behaviour is a trilinear force-elongation diagram. In this latter case, the ultimate elongation (δ_3) was evaluated assuming an arbitrary, but reasonable, axial deformation of the anchor equal to 3% of L_b (Ermopoulos & Stamatopoulos, 1996). The elongation at rupture (δ_4) was determined by arbitrarily assuming a negative slope of the softening branch equal to 20% of the elastic stiffness. The results of the calculation are reported in Table 2. During loading and unloading cycles, the springs exhibit a hysteretic behaviour based on kinematic hardening with pinching. Thus, this joystick model contains material nonlinearities in the springs' behaviour. Other types of nonlinearities considered in the model are loss of contact when springs fail in tension and geometrical nonlinearity with P-Δ effects.

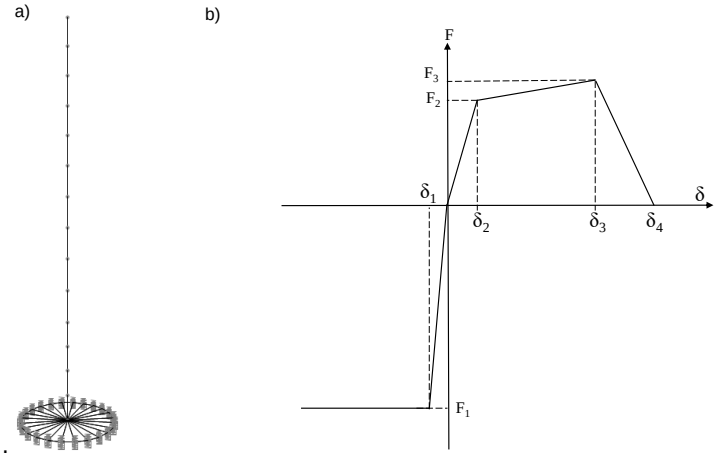

Figure 2: a) Joystick model. b) Force-displacement diagram of the springs of joystick model.

Table 2: Values of the forces and displacements for the springs of the joystick model.

	F_1 [kN]	F_2 [kN]	F_3 [kN]	δ_1 [mm]	δ_2 [mm]	δ_3 [mm]	δ_4 [mm]
Tower-1	-1333	226	254	-0.44	0.90	7.00	12.60
Tower-2	-10094	3298	3710	-1.20	2.75	25.08	42.3

3.2 Analysis

The dynamic analysis strategy followed was the *multi-stripe* analysis (Jalayer, 2003), which typically requires the definition of hazard-consistent seismic input at various levels of ground shaking intensity. The procedure followed for record selection was the conditional spectrum method (Lin et al., 2013), with details on the required hazard models and results provided in Iervolino et al. (2018). Modal analysis resulted in a first-mode period of vibration equal to $T = 0.18\ s$ for Tower-1 and $T = 0.30\ s$ for Tower-2. The conditioning ground motion intensity adopted for both cases was 5%-damped spectral pseudo-acceleration at $T = 0.3\ s$, $Sa(0.3\ s)$. A total of two-hundred records were selected to be divided in ten intensity stripes representing increasing return period of intensity measure exceedance from site-specific probabilistic seismic hazard analysis, to be used for both the investigated case studies. For the definition of a viscous damping matrix, the Rayleigh approach, assigning a damping ratio of 2% to the first and third mode's periods of vibration, was followed.

3.3 Failure criteria

Fragility functions provide the conditional probability of structural failure (F) given a ground motion intensity measure (IM), that is, $P[F|IM]$. Failure, in NaTech context, is defined as structural damage that can provoke the release of the tower's content. Herein, it was assumed that content loss can occur when ground shaking compromises the global stability and/or structural integrity of the tower. This can be the consequence of damage to the connection with the foundation or failure of the supporting steel skirt. Failure of the skirt can occur due to longitudinal buckling (EN 13445-3, 2021) while the connection to the foundation can fail due to tensile rupture of the anchors or the rupture of the welds between the base plate and the skirt.

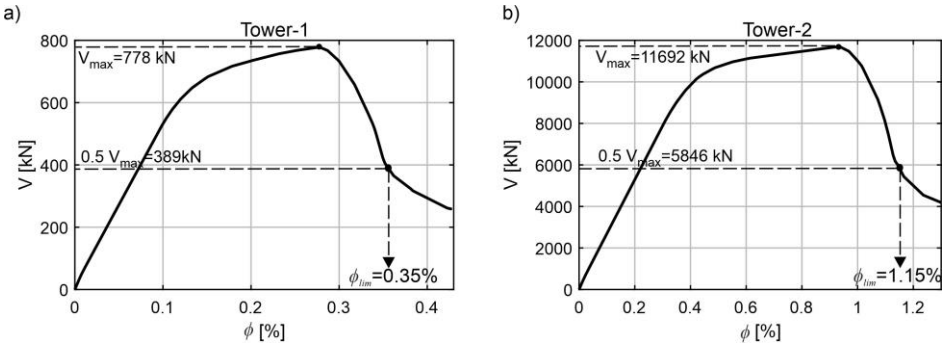

Figure 3: Pushover curves for a) Tower-1, and b) Tower-2.

A set of engineering demand parameters induced by each ground motion were recorded during multi-stripe analysis. Dynamic instability against overturning moment caused by tension failure of a number of anchors was considered to occur when the maximum transient drift value (ϕ) exceeds a limit value (ϕ_{lim}), the former defined as the top displacement to height ratio and the latter as the value corresponding to a $50\ \%$ drop in lateral resistance in terms of base shear $(0.5 \cdot V_{max})$ on the descending branch of the static pushover curve, as shown in Figure 3. This failure criterion was chosen consistent with previous works on seismic structural reliability (Iervolino et al., 2018). The figure shows the results of the static nonlinear analysis for both towers, expressed in terms of base shear (V) – drift (ϕ) diagrams. These pushover curves were obtained using a constant lateral force profile proportional to the first-mode modal load. After a first linear branch, yielding of the anchorage and base plate is characterized by some hardening behavior culminating at a peak base shear V_{max} , whereas a softening branch starts due to gradual rupture of anchors. The difference in V_{max} between the two towers, that can be observed in the figure, is due to the greater mass of the second one, stemming from design requirements of the higher operational pressure which leads to thicker vessel wall thickness.

Failure due to longitudinal buckling of the skirt was evaluated in postprocessing the results of convergent runs, by comparing the meridional compressive stress (σ_c) with the maximum allowable meridional compressive stress $(\sigma_{c,all})$ evaluated according to EN 13445-3 (2021) or equivalently by EN 1993-1-6 (2017), for buckling in the elastic range. A similar approach was followed to evaluate failure due to rupture of the base-to-skirt welds, by comparing the seismic stress demand on the fillet weld (σ_w) at the base of the skirt with the mean capacity at the throat of the weld $(\sigma_{w,all})$, with both demand and capacity stresses of the weld are evaluated following the directional method present inside the EN 1993-1-8 (2005). Non-convergent runs were verified to be the result of failure of almost all anchors and are classified as collapse cases.

4. Results and discussion

Figure 4 shows the results of the multi-stripe analysis carried out for ten values of Sa(T=0.3s) (stripes). For each stripe, twenty records of three-component ground acceleration were applied to the towers. The figure reports

the demand over capacity ratios for the failure criteria considered for the analysis: panels a) and d) show the tower drifts; panels b) and e) the longitudinal buckling of the skirts; and panels c) and f) the failure of the welds at the base. The number of dynamic instabilities encountered is conventionally reported on the right vertical axis. No dynamic instability was observed for Tower-2, while for Tower-1 there were 7 such cases at the tenth stripe. Tower-1 exhibits higher ϕ/ϕ_{lim} than Tower-2 for each stripe, which is to be expected because the higher-pressure vessel of Tower-2 requires detailing with thicker skirt and base plate. On the other hand, Tower-2 has larger $\sigma_c/\sigma_{c,all}$ and $\sigma_w/\sigma_{w,all}$ ratios than Tower-1.

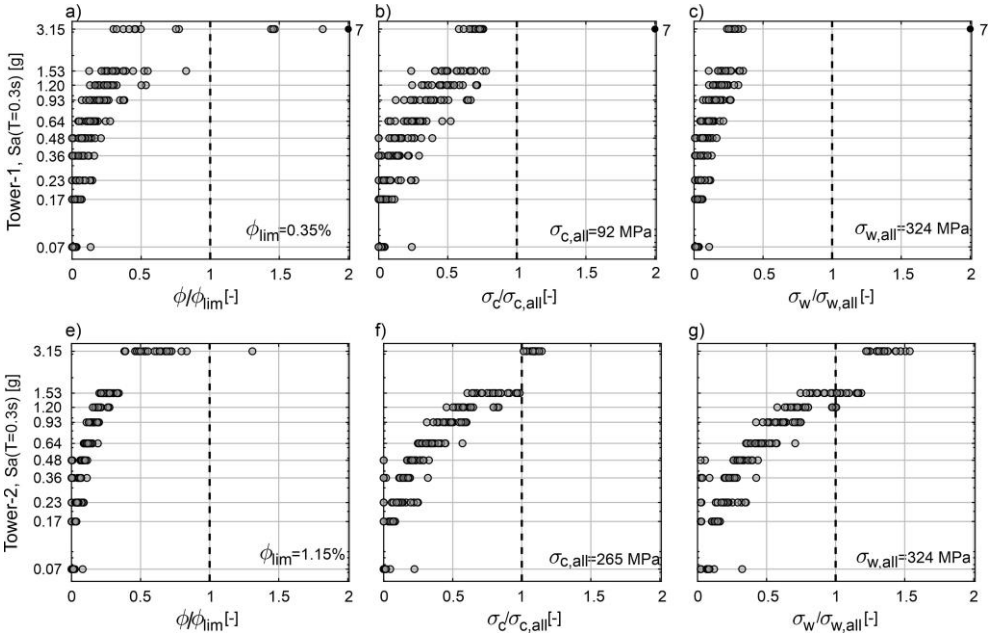

Figure 4: Results of multi-stripe analysis for: a), e) drift; b), f) longitudinal buckling of the skirt; c) and g) failure of the welds. The first row shows the results for Tower-1 and the second row, the results of Tower-2.

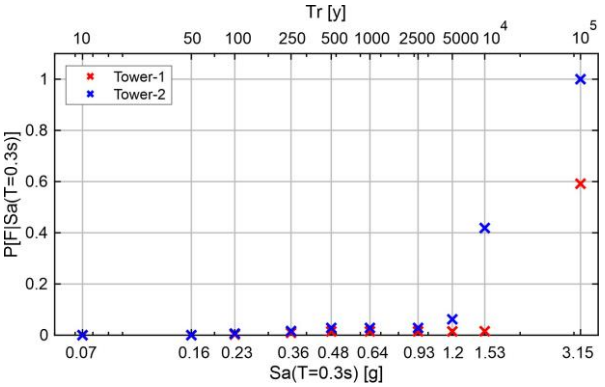

Figure 5: Conditional probabilities of failure given seismic intensity.

These three ratios were summarized into a single engineering demand parameter of demand over capacity, $D/C = max\{\phi/\phi_{lim}, \sigma_c/\sigma_{c,all}, \sigma_w/\sigma_{w,all}\}$. Subsequently, the conditional failure probability $P[F|IM] = P[F|Sa(0.3s)] = P[D/C > 1|Sa(0.3s)]$ was estimated for each intensity level (stripe) by fitting a lognormal model for D/C on the sample of responses from convergent analyses, via the algorithm implemented in Baraschino et al. (2020). These conditional probabilities of failure are shown in Figure 5. The figure shows that the failure probability estimates for Tower-2 exceed those of Tower-1, due to the higher normalized compressive stress demand on the support skirt and the stress of the skirt-to-base-plate fillet weld of Tower-2. This difference in seismic behavior between the two towers is partly due to the difference in mass, resulting from different operating pressures. It should be therefore noted that, apart from the difference in fragility, the consequences due to contents release from structural collapse of the two towers, could also vary due to the difference in operating pressure of said contents. A potential comparison of the Tower-1 results could be made with the study of Karaferis et al. (2022) who analyzed a process tower of similar height, but smaller pressure vessel diameter by almost half. In that study a lognormal fragility is provided, in terms of peak ground acceleration (PGA), for

the shell buckling case, allowing some form of comparison. Due to the different conditioning intensity measures in the two studies, direct comparison of the conditional failure probabilities is not possible. However, one may compare reliability estimates for the site of Ravenna, by integrating the fragility values with site-specific PGA and Sa(0.3s) hazard curves, according to the procedure described in (Iervolino et al. 2018) to obtain annual failure rates, λ_f. This operation, using the results of the present study, yields λ_f=1.65E-4, while the results from the aforementioned work give λ_f=3.96E-4, indicating that different process towers with similar geometrical characteristics, can have seismic reliabilities that vary due to other parameters.

5. Conclusions

This paper presents a modelling approach to derive the fragility functions for steel process towers under seismic action. The numerical models account for the non-linear behavior of the base-to-foundation connection of the towers, but neglect potential interactions with converging pipelines. The conditional probabilities of failure were derived via nonlinear dynamic analysis, using a multi-stripe approach, for failure criterions that conventionally correspond to structural damage causing loss of content. It was observed that the tower with lower operating pressure, and hence lower vessel mass, exhibited higher drift demands with respect to its capacity, while the tower with higher pressure and mass was more susceptible to weld failures and longitudinal buckling of the skirt.

Acknowledgments

The study presented was developed within the RETURN “Multi-risk science for resilient communities under a changing climate” (National Recovery and Resilience Plan-NRPP, Mission 4, Component 2, Investment 1.3 – D.D. n.341 15/3/2022, PE0000005); and within the activities with ReLUIS-DPC (Rete di Laboratori d’Ingegneria Sismica—Dipartimento di Protezione Civile) 2022−2024 research agreement, funded by the Italian Department of Civil Protection.

References

Antonioni G., Spadoni G., Cozzani V., 2007, A methodology for the quantitative risk assessment of major accidents triggered by seismic events, Journal of Hazardous Materials, 147(1–2), 48–59.

Baraschino R., Baltzopoulos G., Iervolino, I., 2020, R2R-EU: Software for fragility fitting and evaluation of estimation uncertainty in seismic risk analysis, Soil Dynamics and Earthquake Engineering, 132.

Brunelli G., Borgognoni F., 2014, Seismic assessment of industrial process equipment, Impiantistica Italiana, (in Italian).

CS.LL.PP., 2018, Ministerial Decrete: Technical Standards for Construction (NTC 2018), Gazzetta Ufficiale della Repubblica Italiana, n.42, 20 febbraio, Suppl. Ordinario n.8 Ist. Polig. e Zecca dello Stato S.p.a., Rome, Italy (in Italian).

Ermopoulos J. C., Stamatopoulos G. N., 1996, Mathematical Modelling of Column Base Plate Connections, In J. Construct, Steel Res, 36 (2).

Fabbrocino G., Iervolino I., Orlando F., Salzano E., 2005, Quantitative risk analysis of oil storage facilities in seismic areas, Journal of Hazardous Materials, 123(1–3), 61–69, doi.org/10.1016/j.jhazmat.2005.04.015.

Iervolino I., 2003, Seismic quantitative risk analysis in the process industry, PhD Thesis, University of Naples Federico II, Naples, Italy (in Italian).

Iervolino I., Spillatura A., Bazzurro P., 2018, Seismic Reliability of Code-Conforming Italian Buildings. Journal of Earthquake Engineering, 22, 5–27, doi.org/10.1080/13632469.2018.1540372.

Jalayer F., 2003, Direct Probabilistic Seismic Analysis: Implementing Non-Linear Dynamic Assessments, PhD Thesis, Stanford University Institute of civil and environmental engineering, Stanford, USA.

Karaferis N. D., Kazantzi A. K., Melissianos V. E., Bakalis K., Vamvatsikos D., 2022, Seismic fragility assessment of high-rise stacks in oil refineries, Bulletin of Earthquake Engineering.

Krausmann E., Cozzani V., Salzano E., Renni E., 2011, Industrial accidents triggered by natural hazards: An emerging risk issue, Natural Hazards and Earth System Science, 11(3), 921–929.

Lin T., Haselton C. B., Baker J. W., 2013, Conditional spectrum-based ground motion selection. Part I: Hazard consistency for risk-based assessments, Earthquake Engineering & Structural Dynamics, 42(12), 1847–1865.

Moharrami H., Amini M. A., 2014, Seismic vulnerability assessment of process towers using fragility curves, Structural Design of Tall and Special Buildings, 23(8), 593–603, doi.org/10.1002/tal.1067.

UNI EN 1991-1-4, 2004, Eurocode 1 - EN 1991-1-4-2004 - General actions - Wind actions.

UNI EN 1993-1-6, 2017, Eurocode 3, Design of steel structures - Part 1-6: Strength and stability of shell structures.

UNI EN 1993-1-8, 2005, Eurocode 3 - Design of steel structures - Part 1-8: Design of joints.

UNI EN 1998-1, 2013, Eurocode 8 - Design of structures for earthquake resistance - Part 1: General rules, seismic actions and rules for buildings.

UNI EN 13445-3, 2021, Unfired pressure vessels - Part 3: Design.